Heavy Ions Radiation Effects on 4kb Phase-Change Memory

Anna Lisa Serra, Tobias Vogel, Gauthier Lefevre, Stefan Petzold, Nico Kaiser, Guillaume Bourgeois, Marie-Claire Cyrille, Lambert Alff, Christina Trautmann, Christophe Vallée, et al.

Heavy Ions Radiation Effects on 4kb Phase-Change Memory

A. L. Serra[1], T. Vogel[2], G. Lefevre[3], S. Petzold[2], N. Kaiser[2], G. Bourgeois[1], M. C. Cyrille[1], L. Alff[2], C. Trautmann[4], C. Vallée[3], D. Sylvain[3], C. Charpin-Nicolle[1], G. Navarro[1] and E. Nowak[1]

***Abstract*— In this work we analyze, thanks to both material and 4kb memory arrays characterization, the different effects of heavy ion radiation at high fluences on $Ge_2Sb_2Te_5$ and Ge-rich GeSbTe based Phase-Change Memory (PCM).**

***Index Terms*— Radiation hardness, radiation effects, phase-change memory, PCM, $Ge_2Sb_2Te_5$, Ge-rich GeSbTe, interfacial layer PCM.**

I. Introduction

PHASE-Change Memory (PCM) is considered today the most mature and promising resistive memory technology, as demonstrated by recent commercialization for Storage Class Memory market, because of its scalability and proven reliability [1]. Its functionality is based on the reversible transition of a chalcogenide material that can be switched theoretically infinite times between the amorphous and the crystalline phase. The crystalline phase is ordered and low resistive, whereas the amorphous phase is disordered and highly resistive. The temperature at which the transition takes place, called crystallization temperature (T_C), can be tuned by engineering the material composition [2]. This enables the improvement of the PCM thermal stability, in particular targeting automotive application which requires strict reliability specifications at high temperature [3]. In a PCM device, the programming is achieved thanks to the voltage (i.e. current) induced Joule heating of the phase-change material that enables the phase transition. Dependently on the programming electrical pulse parameters (i.e. intensity, duration etc.), the phase-change material can be melt-quenched in the amorphous phase (RESET state), or gradually recrystallized (SET state). The most common used phase-change material is $Ge_2Sb_2Te_5$ (GST), featuring a fast phase transition and a high resistance window (i.e. ratio between the amorphous and the crystalline resistivity). However, GST has a T_C of ~ 150 °C, not compatible with automotive requirements. Recent material engineering leaded to the development of a Ge-rich GeSbTe (GGST) alloy capable of high temperature amorphous stability, that made PCM suitable also for automotive applications [4].

Since the discovery of phase-change materials and PCM [5], being the storage mechanism not based on charge storage (like in flash memory technology), a high radiation tolerance was foreseen. Indeed, the first studies on the radiation tolerance of PCM arrays demonstrated the PCM device radiation hardness to different kind of ion beams, highlighting that degradation is mainly given by the impact on the CMOS selector device, due to charges trapped in the gate [6] [7] [8]**.** Nevertheless, further studies described some possible degradation mechanisms due to radiation that could impact the PCM depending on its device structure, in particular in highly scaled devices [9] [10].

The aim of this work is to investigate the heavy-ion radiation effects in state-of-the-art "Wall-based" PCM devices [11] comparing standard GST with GGST. Firstly, morphological evolution of both amorphous and crystalline phases of the chalcogenide material under heavy ion irradiation at different fluences are analyzed by X-ray diffraction (XRD) and TEM/EDX analyses. Then, SET and RESET states evolution under different irradiation fluences in 4kb arrays is presented demonstrating a higher radiation tolerance of GGST wrt GST. Finally, a standard PCM stack is compared with an innovative interfacial layer PCM stack (IL-PCM) [12], showing the higher radiation tolerance of IL-PCM, likely due to its nm-scale active region.

II. Radiation Effects on GeSbTe Alloys Structure

The evolution of amorphous (as-deposited) and crystalline (obtained by annealing at 450 °C for 15 min) structures of

This work was partially funded by European commission, French State and Auvergne-Rhône Alpes region through ECSEL project WAKEMEUP and French Nano2022 program.

The work leading to this publication has received funding within the ECSEL Joint Undertaking project WAKeMeUP in collaboration with the European Union's H2020 Framework Program (H2020/2014-2020) and National Authorities, under grant agreement number 783176. Funding by the Federal Ministry of Education and Research (BMBF) under contract 16ESE0298 and by the DFG grant AL 560/21-1 is gratefully acknowledged. The irradiation experiments for this publication were performed at the UNILAC X0 beam line at the GSI Helmholtz Center for Heavy Ion Research, Darmstadt (Germany), based on a UMAT experiment in the frame of FAIR Phase-0.

[1] CEA, LETI, MINATEC Campus, F-38054 Grenoble, France and Univ. Grenoble Alpes, F-38000 Grenoble, France (e-mail: annalisa.serra@cea.fr, christelle.charpin@cea.fr, gabriele.navarro@cea.fr, etienne.nowak@cea.fr).

[2]Department Advanced Thin Film Technology, Institute of Materials Science, Technische Universität Darmstadt, 64287 Darmstadt, Germany (e-mail: stefan.petzold@tu-darmstadt.de, tobias.vogel@tu-darmstadt.de, lambert.alff@tu-darmstadt.de, nico.kaiser@tu-darmstadt.de)

[3]CNRS-LTM Laboratoire des Technologies de la Microélectronique, 38054 Grenoble, France (e-mail: gauthier.lefevre@cea.fr)

[4]Materials Research Department, GSI Helmholtzzentrum fuer Schwerionenforschung, 64291 Darmstadt, Germany and Institute of Materials Science, Technische Universität Darmstadt, 64287 Darmstadt, Germany (e-mail: c.trautmann@gsi.de)

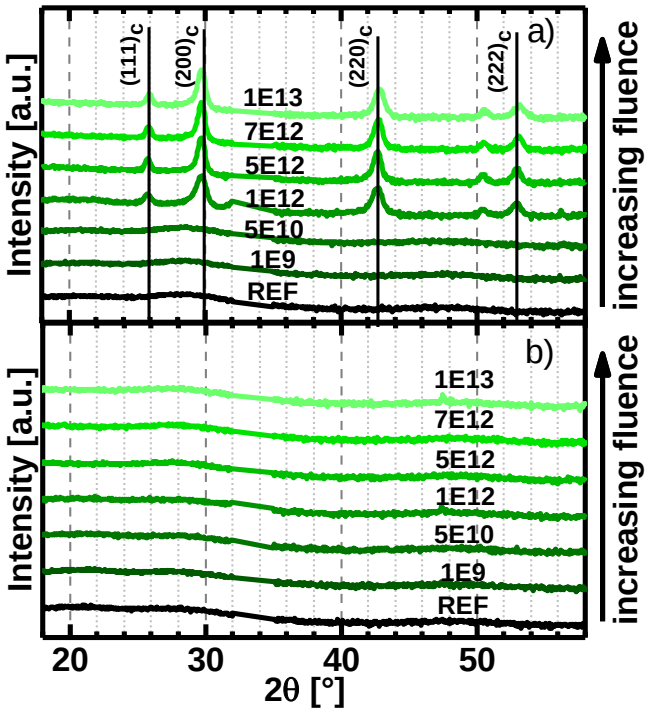

Fig. 1 XRD patterns of GST (a) and GGST (b) amorphous layers before (REF) and after irradiations at increasing fluence (reported in the spectra in ions/cm^2). XRD peaks corresponding to GST cubic phase are highlighted.

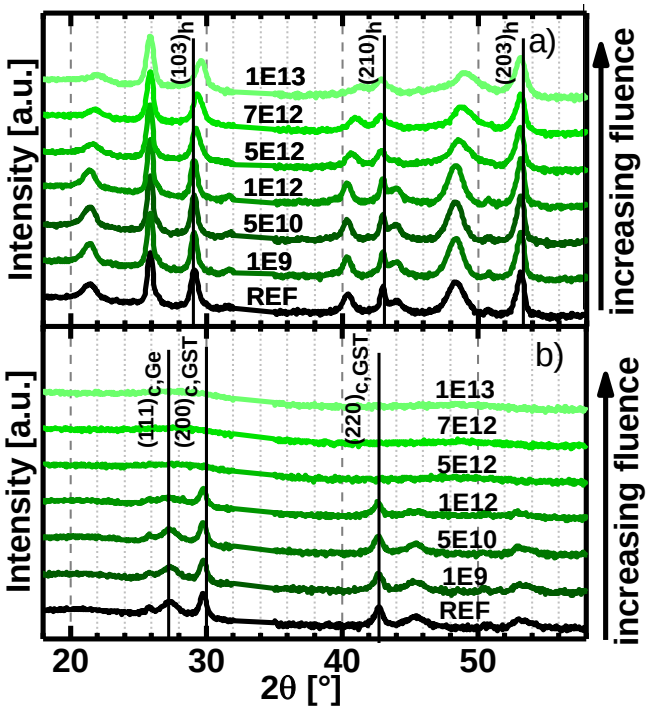

Fig. 3 XRD patterns of GST (a) and GGST (b) crystalline layers (after annealing at 450 °C 15min) before (REF) and after irradiations at increasing fluence (reported in the spectra in ions/cm^2). XRD peaks corresponding to the GST hexagonal phase (h,GST) are highlighted in (a) and GST cubic (c,GST) and Ge cubic (c,Ge) phase in (b).

phase-change layers under ion beam irradiation was investigated by XRD and TEM/EDX analyses. The 100 nm thick films were deposited on Si substrate and protected from air exposure by a 10 nm SiN encapsulation layer. The samples were irradiated with Au ions with an energy of 1.635 GeV at different fluences (from 10^9 up to 10^{13} ions/cm^2) with a constant flux of 3×10^8 ions/(cm^2 s). Heavy-ion irradiation experiments were performed at the beam facility of GSI Darmstadt (Germany).

A. Amorphous layers analysis

The evolution of the GST and GGST structures with increasing beam fluence is reported in **Fig. 1.** The analysis shows a crystallization of GST toward a cubic phase between 5×10^{10} and 10^{12} ions/cm^2 (**Fig. 1 (a)**). The crystallization triggered at high fluences is confirmed by TEM and nano-diffraction patterns analyses reported in **Fig. 2**, revealing the growth of large crystals in the system, compatibly with the sharpness of the XRD peaks detected. We think that two main mechanisms are competing in the material structure under ions irradiation: i) the breaking of crystalline bonds; ii) a localized temperature increase that could induce nucleation and growth phenomena (if the temperature reached is higher than the T_C). XRD results for GST seems to confirm that the second mechanism is predominant at the investigated fluences. In GGST, on the contrary, the amorphous phase is preserved even at high fluences, confirming the higher thermal stability of the material.

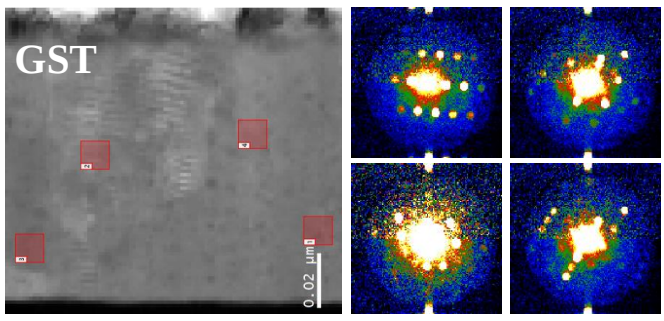

Fig. 2 TEM (left) and nano-diffraction patterns (right) analyses of as-deposited amorphous GST after irradiation at a fluence of 10^{13} ions/cm^2. It evidences the creation of a crystalline structure with large crystalline grains.

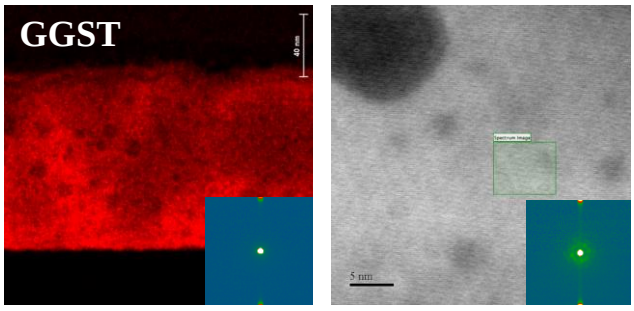

Fig. 4 TEM/EDX and nano-diffraction patterns analyses of crystalline GGST after irradiation at a fluence of 7×10^{12} ions/cm^2. We observe the Ge segregation, induced by annealing, remained unchanged after irradiation (left). The main irradiation impact is on the crystalline morphology with the reduction at nm scale of the crystals size, as evidenced by few and low intensity nano-diffraction patterns identified (right).

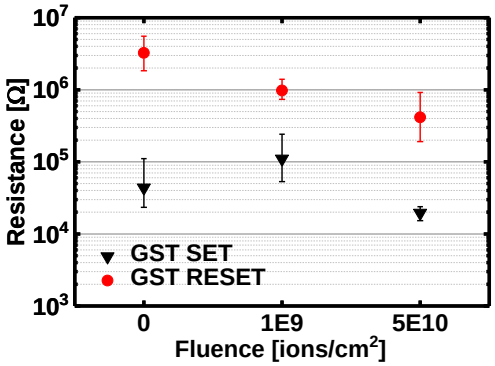

Fig. 5 Median and ±σ for SET and RESET distributions in GST 4kb arrays before and after irradiations at increasing fluences.

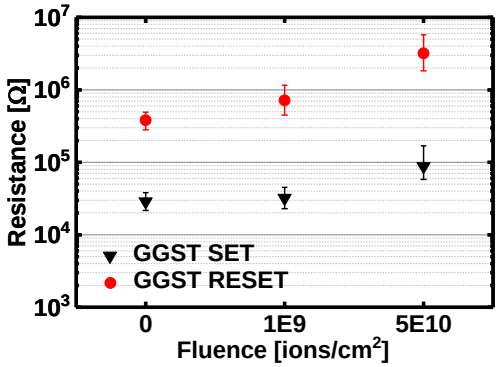

Fig. 6 Median and ±σ for SET and RESET distributions in GGST 4kb arrays before and after irradiations at increasing fluences.

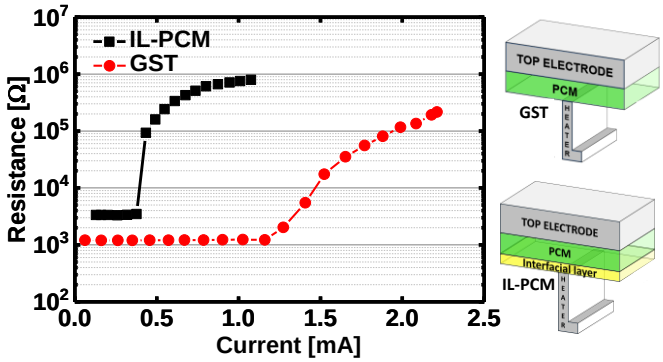

Fig. 7 Resistance-vs-Current characteristics comparing a standard GST device with an IL-PCM. IL-PCM shows a high current reduction wrt GST in devices featuring same critical dimension (electrode area $\sim 3 \times 10^{-3}$ µm²).

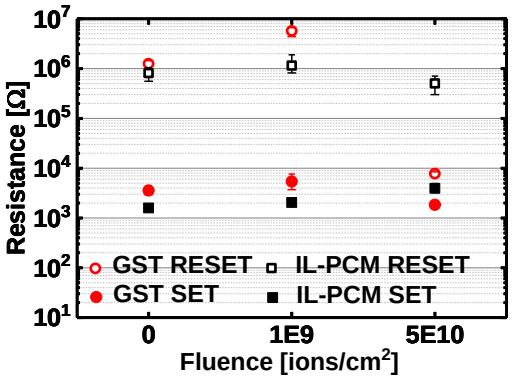

Fig. 8 Median and ±σ for SET and RESET distributions in GST and IL-PCM 4kb arrays before and after irradiations at increasing fluences.

B. Crystalline layers analysis

Fig. 3 shows the XRD patterns of GST and GGST layers annealed at 450 °C. The annealing brings the GST in the hexagonal phase (h) that is preserved (**Fig. 3 (a)**) up to high fluences. However, at 5×10^{12} ions/cm² we observe a broadening and shift of the hexagonal peaks, confirming the competition between bonds breaking and recreation. In GGST (**Fig. 3 (b)**), from 10^{12} ions/cm², we observe a gradual vanishing of the Ge and GST cubic peaks present after the annealing (known to induce phase separation in GGST).

TEM/EDX analysis (**Fig. 4**) performed on the irradiated samples confirms the preservation of the segregated morphology of GGST even after irradiation. However, almost no crystalline patterns are detected. By pushing nano-diffraction patterns analysis at its limit, we can highlight few and low signal nm-scale features, confirming a residual polycrystalline nature of both Ge and GeSbTe phases, extremely impacted by irradiation at high fluences. The preserved short range order in the layer, can be the origin of the XRD feature observed between 25° and 35°, present also in several chalcogenide amorphous layers. The impact of irradiation on GGST crystalline samples, can be interpreted as a confirmation of the higher bonds breaking rate wrt nucleation and growth rates in this layer, being the crystallization slower in GGST wrt standard GST (i.e. at the origin of GGST higher thermal stability).

III. Radiation Effects on 4kb PCM

We studied the radiation effects on state-of-the-art wall-based PCM devices [11] embedded in the Back-End-Of-the-Line (BEOL) fabrication of 4kb arrays integrated in LETI Memory Advanced Demonstrator (MAD) based on 130 nm CMOS technology. The behavior of both GST and GGST-based PCM are investigated and compared before and after irradiations at different fluences. Moreover, the standard GST stack is compared in terms of radiation tolerance with an innovative IL-PCM [12]. PCM arrays programmed in both SET and RESET state are read after irradiation experiments at fluences of 10^9, 5×10^{10} and 10^{12} ions/cm², with same experimental conditions described in previous chapter. All the arrays irradiated at 10^{12} ions/cm² showed the impossibility to access to the PCM cells after the experiment, due to the strong impact of heavy ions on the addressing circuitry. It is important to note that in this work the use of high fluences in a short time induces a higher damage of CMOS devices and external circuitry wrt a harsh radiation environment situation where the fluence is generally smaller [7]. All the data are then reported for the two lower fluences used.

A. GST vs GGST

The median and ±σ for the SET and RESET distributions measured in GST and GGST arrays are reported in **Fig. *5*** and **Fig. *6***. The analysis is performed on devices with an electrode

area of 10^{-3} µm^2. The SET state in GST faces a structural relaxation at a fluence of 10^9 ions/cm^2, highlighted by the increase of the resistance, whereas it shows a reduction (i.e. recrystallization) at a resistance comparable with the initial one at 5×10^{10} ions/cm^2. This is in agreement with the incoming crystallization observed in the material analysis at high fluences. The loss of the programmed state is more evident in the GST RESET resistance value that decreases with increasing fluence, due to the incoming crystallization of the amorphous phase. On the contrary, both SET and RESET states in GGST show only structural relaxation (known to be higher wrt GST) at both fluences. The higher thermal stability of GGST hinders the crystallization phenomena and the loss of information even at a fluence of 5×10^{10} ions/cm^2. Indeed, both the resistance window and the amorphous phase in the RESET state result to be preserved.

B. GST vs IL-PCM

Finally, we compared the radiation tolerance of a standard GST stack with an innovative IL-PCM stack integrated in wall devices featuring an electrode area of 3×10^{-3} µm^2. The advantageous lower programming current in IL-PCM is highlighted in **Fig. *7***, achieved thanks to the intrinsic active volume reduction in this structure. IL-PCM shows a higher radiation tolerance wrt GST (**Fig. *8***). Indeed, while the SET state remains stable in both stacks at all fluences, the RESET state shows a complete recrystallization at 5×10^{10} ions/cm^2 with the loss of the resistance window in standard GST stack. IL-PCM on the contrary preserves a good resistance window even at the highest fluence. Indeed, a higher thermal stability is expected in reduced amorphous chalcogenide volumes, due to a reduced nucleation rate. Moreover, the reduced electrode effective surface of an IL-PCM, makes the device less sensible to local heating phenomena that could be induced by ion interactions with the electrode/phase-change material interface [10] [8].

IV. CONCLUSIONS

We compared radiation tolerance of GST and GGST phase-change materials. From physico-chemical analyses on irradiated amorphous and crystalline layers, we highlighted the two main competitive mechanisms induced by irradiation: bonds breaking and crystallization induced by local temperature increase. In GST we observe a dominant crystallization at high fluences, while GGST, being more thermally stable, features a higher structural relaxation and a gradual reduction of the long range order, demonstrated by the gradual loss of the crystalline structure. Thanks to state-of-the-art 4kb PCM array analysis, we demonstrated the higher radiation tolerance of GGST devices, showing no recrystallization of the amorphous phase (RESET) even at high fluence of 5×10^{10} ions/cm^2. Finally, we report the radiation hardness of the IL-PCM stack solution wrt standard GST, confirming the benefit of a reduced PCM device size against heavy ion irradiation impacts.

REFERENCES

[1] Huai-Yu Cheng et al., "3D cross-point phase-change memory for storageclass memory", J. Phys. D: Appl. Phys. 52 (2019).

[2] G. Navarro et al., "Phase-Change Memory:Performance, Roles and Challenges", 2018 IEEE International Memory Workshop.

[3] F. Arnaud et al., "Truly Innovative 28nm FDSOI Technology for Automotive Micro-Controller Applications embedding 16MB Phase Change Memory", 2018 IEEE International Electron Devices Meeting (IEDM).

[4] P. Zuliani et al., "Engineering of chalcogenide materials for embedded applications", Solid-State Electronics, 111 (2015) 27-31.

[5] S. R. Ovshinsky et al., "Radiation Hardness of Ovonic Devices, Energy Conversion Devices".

[6] N. Wrachien et al., "Total Ionizing Dose Effects on 4 Mbit Phase Change Arrays", IEEE Transactions on Nuclear Science, 2008.

[7] A. Gasperin et al., "Analysis of Proton and Heavy-Ion Irradiation Effects on Phase Change Memories With MOSFET and BJT Selectors", 2008, vol. 55, no. 6.

[8] S. Gerardin et al., "Present and Future Non-Volatile Memories for Space", IEEE Transactions on nuclear science, vol. 57, no.6, 2010.

[9] S. Gerardin et al., "Single Event Effects in 90-nm Phase Change Memories", IEEE Transactions on Nuclear Science, vol. 58, no. 6, 2011.

[10] S. Gerardin et al.,"Upsets in Phase Change Memories Due to High-LET Heavy Ions Impinging at an Angle", IEEE Transactions on nuclear science, vol. 61, no. 6, 2014.

[11] A. L. Serra et al.,"Outstanding Improvement in 4Kb Phase-Change Memory of Programming and Retention Performances by Enhanced Thermal Confinement", 2019 IEEE International Memory Workshop (IMW).

[12] G. Navarro et al., "Innovative PCM+OTS Device with High Sub-Threshold Non-Linearity for Non-Switching Reading Operations and Higher Endurance Performance", VLSI 2017.